IEEE Access
Multidisciplinary | Rapid Review | Open Access Journal

Received January 1, 2020, accepted January 17, 2020, date of publication February 4, 2020, date of current version February 14, 2020.

Digital Object Identifier 10.1109/ACCESS.2020.2971624

Multitarget Tracking Using One Time Step Lagged Delta-Generalized Labeled Multi-Bernoulli Smoothing

GUOLONG LIANG[1,2,3,4], QUANRUI LI[1,2,3], BIN QI[1,2,3,4], AND LONGHAO QIU[1,2,3,4]

[1]Acoustic Science and Technology Laboratory, Harbin Engineering University, Harbin 150001, China
[2]College of Underwater Acoustic Engineering, Harbin Engineering University, Harbin 150001, China
[3]Key Laboratory of Marine Information Acquisition and Security, Harbin Engineering University, Harbin 150001, China
[4]Qingdao Haina Underwater Information Technology Company Ltd., Qingdao 266500, China

Corresponding author: Bin Qi (qibin@hrbeu.edu.cn)

This work was supported in part by the National Key Research and Development Plan under Grant 2017YFC0306900, in part by the Basic Technical Research Project under Grant JSJL2016604B003, and in part by the Equipment Pre-research of Acoustic Science and Technology Laboratory "Underwater Weak Target Detection and Multitarget Tracking Key Technology Research" under Grant 6142109180207.

ABSTRACT Aiming at improving the tracking performance of the delta-generalized labeled multi-Bernoulli (δ-GLMB) filter, we present a one time step lagged δ-GLMB smoother in this work, which also inherently outputs targets trajectories and differs from the Probability hypothesis density (PHD), Multi-Bernoulli (MB), and Cardinalized probability hypothesis density (CPHD) smoothers that are incapable of generating target trajectories directly. Under the standard multitarget measurement likelihood and state transition kernel, we show that a δ-GLMB distributed multitarget filtering density would result in a same distributed one time step lagged multitarget smoothing density. An efficient implementation of the proposed smoothing algorithm using the standard ranked assignment technique is also given. Numerical results show that the proposed smoother is capable of tracking a time-varying number of targets, in the presence of measurement origin uncertainty, target detection uncertainty, and clutter, and show that the proposed smoother outperforms the δ-GLMB filter, and the PHD, MB, and CPHD smoothers of the same time lag on both the estimates of target number and state and it also outperforms the LMB and the approximated δ-GLMB smoothers of the same time lag on target number estimate.

INDEX TERMS Delta-generalized labeled multi-Bernoulli, multitarget tracking, random finite set, smoothing.

I. INTRODUCTION

The objective of multitarget tracking (MTT) is to estimate the number of targets and their states jointly using measurements provided by sensors, such as radar, sonar, and infrared [1], [2]. Driven by aerospace applications [3], MTT has also found applications in other areas such as image processing [4], automatic vehicles [5], biomedical research [6], etc. The main challenges in MTT are various uncertainties, such as measurement origin uncertainty, target detection uncertainty, and target number uncertainty [1], [2].

To handle the uncertainties in MTT, a lot of approaches [1]–[3], [7] have been proposed. To date, three major approaches to MTT exist. They are multiple hypothesis tracking (MHT) [8], joint probabilistic data association (JPDA) [9], and random finite set (RFS) [7]. The RFS approach provides a systematic and elegant Bayesian formulation for MTT, in which the collection of target state is treated as an RFS.

The core of the RFS approach is the Bayes multiobject filter [7], which recursively propagates the multiobject filtering density forward in time. However, due to its numerical complexity, the optimal Bayes multiobject filter is generally computationally intractable [7]. Approximations such as the probability hypothesis density (PHD) filter [10], cardinalized PHD (CPHD) filter [11], multi-Bernoulli filters [7], [12], and the more recently Poisson multi-Bernoulli mixture (PMBM) filter [13], [14] have been proposed as tractable solutions.

The associate editor coordinating the review of this manuscript and approving it for publication was Wen Chen.

This work is licensed under a Creative Commons Attribution 4.0 License. For more information, see http://creativecommons.org/licenses/by/4.0/

Nevertheless, these Bayes multiobject filters do not produce trajectory estimates directly, and they need other techniques, such as [15] for the PHD filter, to acquire trajectory estimates.

Based on the labeled RFS [16], a Bayes multitarget tracking filter called delta-generalized labeled multi-Bernoulli (δ-GLMB) filter was proposed in [17]. The δ-GLMB filter models the targets states using labeled RFS, which makes the targets states distinguishable across multiple time steps and leads to its trajectory generation capability. It is a computationally tractable exact-closed-form solution of the multitarget Bayes filter [18]. The δ-GLMB filter rests on the premise that the δ-GLMB density is a multiobject conjugate prior with respect to the multitarget measurement likelihood and is also closed under the Chapman-Kolmogorov prediction equation [16]. Implementation that avoids the super-exponentially growing number of filtering components is given in [17]. A computational efficient implementation of the δ-GLMB filter that combines the prediction and update into a single step is detailed in [19]. Principled approximations of the δ-GLMB filter that preserve the key statistical properties of the full multitarget density were also proposed to further reduce the numerical complexity, which includes the labeled multi-Bernoulli (LMB) filter [20] and the marginalized δ-GLMB filter [21]. The δ-GLMB filter has inspired much work, such as multitarget tracking with merged measurements [22], extended target [23], and generic observation model [24]. More recently, unlabeled solutions that also output targets trajectories using the so-called sets of trajectories are also presented [25], [26]. Those Bayes multiobject filters such as the PHD [10], CPHD [11], MB [12], and δ-GLMB [16] filters obtain their filtering densities at a given time using measurements only up to that time.

By utilizing measurements beyond a given time, smoothing generally yields better estimate than filtering [27]. Multiobject smoothing is generally more challenging [28] than single-object smoothing due to the various uncertainties in MTT mentioned above. Principled approximations of the Bayes multiobject smoothers have also been proposed. The PHD smoother was derived using the physical-space approach [29], and it was then derived rigorously using finite set statistics (FISST) [28]. A forward-backward multi-Bernoulli (MB) smoother for multi-target tracking was given in [30], in which they state that it improves the estimation accuracy of target number and state over the MB filter [12]. A tractable but approximate CPHD smoother was proposed in [31], and they show that the CPHD smoother provides better cardinality estimate compared to the PHD smoother and does not exhibit undesirable track deletions that the PHD smoother suffers [31]. However, due to the mathematical formulation of the states, these Bayes multiobject smoothers also do not inherently produce targets trajectories.

Concerning multitarget smoothing using labeled RFS, a generalized labeled multi-Bernoulli forward-backward smoother was derived in [32], but the smoother has not been implemented and no simulation results are given. A computationally efficient LMB smoother was proposed in [33], and they show that it improves the tracking performance over the PHD and MB smoothers, and the LMB filter. A GLMB tracker with partial smoothing was detailed in [34], in which they update the trajectory tuples using the output of the GLMB filter at each time step, and then perform single-object forward-backward smoothing. An approximate δ-GLMB (δ-GLMB-A) smoother was proposed in [35], in which the derivation assumes that no targets births and deaths occur in the smoothing period.

In this work, aiming at improving the tracking performance of the δ-GLMB filter, namely improving the estimates of target number and state, we present a one time step lagged Bayes multitarget smoother using the δ-GLMB density. It is the subsequent work of [35], where the assumption that targets births and deaths do not occur in the smoothing process is removed. In specific, we first show that the one time step lagged multitarget smoothing can be achieved in a way resembles the measurement update of the Bayes multitarget filter [17], and then we show that a δ-GLMB distributed multitarget filtering density would results in a same distributed one time step lagged multitarget smoothing density. We also show that if the birth process follows an LMB RFS, then the implementation of the proposed smoother can be accomplished in an efficient manner by using the ranked assignment technique. Simulation results show that the proposed smoother outperforms the δ-GLMB filter, and the PHD [28], MB [30] and CPHD [31] smoothers of the same time lag on both the estimates of target number and state, and compared to the LMB and δ-GLMB-A smoothers of the same time lag, the proposed smoother provides similar performance on estimate of target state, yet better estimate on target number.

The rest of the paper is organized as follows. Section II first provides a brief review of the two commonly used labeled RFSs, namely the δ-GLMB and LMB RFSs, and then presents the standard multitarget measurement likelihood and the multitarget transition kernel. Closed-form formulation of the proposed smoother is detailed in Section III. Implementation details are presented in Section IV. Section V reports the simulation and experiment results. Concluding remarks and future research direction are presented in Section VI.

II. BACKGROUND

In this work, we adhere to the notation [16] that single-object states are denoted by lowercase letters, e.g. x, $\mathbf{x}$, while multiobject states are denoted by uppercase letters, e.g. X, $\mathbf{X}$, symbols for labeled states and their distributions are bolded to distinguish them from unlabeled ones, e.g. $\mathbf{x}$, $\mathbf{X}$, $\boldsymbol{\pi}$, etc. Spaces are denoted by blackboard bold, e.g. $\mathbb{X}$, $\mathbb{L}$, $\mathbb{Z}$, etc. Also, the multiobject exponential is denoted by $h^X = \prod_{x\in X} h(x)$, where h is a real-valued function, with $h^{\varnothing} = 1$ by convention, and we also denote the generalized Kroneker delta and inclusion functions by

$$\delta_Y^{(X)} = \begin{cases} 1, & \text{if } X = Y \\ 0, & \text{otherwise,} \end{cases} \quad 1_Y^{(X)} = \begin{cases} 1, & \text{if } X \subseteq Y \\ 0, & \text{otherwise} \end{cases}$$

TABLE 1. Summary of frequently used symbols.

Symbol	Interpretation
h^X	Multiobject exponential
$\delta_Y^{(X)}$	Generalized Kroneker delta function
$1_Y^{(X)}$	Generalized inclusion function
$\Delta_{\mathbf{X}}$	Distinct label indictor
$\mathcal{L}_{\mathbf{X}}$	Label set of multitarget state $\mathbf{X}$
$g(Z\,\vert\,\mathbf{X})$	Multitarget measurement likelihood
$g(Z_+\,\vert\,\mathbf{X})$	Multitarget pseudo measurement likelihood
$\mathbf{f}(\mathbf{X}_+\,\vert\,\mathbf{X})$	Multitarget state transition kernel
$(x,\ell)\,,(x_+,\ell_+)$	Labeled states at the current, and next time steps
$g(z\,\vert\,x,\ell)$	Single-target likelihood
$f(x_+\,\vert\,x,\ell)$	Single-target state transition density
(I,ξ)	Filtering hypothesis
(I,ξ,B_+,S_+,θ_+)	Smoothing hypothesis
B_+	Newborn label set
S_+	Surviving label set
θ_+	Association map

To aid the reader, a summary of the frequently used symbols in this work is given in Table 1 below.

A labeled RFS is an RFS [7] whose elements are assigned with distinct labels [16]. Given state space $\mathbb{X}$, discrete label space $\mathbb{L}$, and projection $\mathcal{L}:\mathbb{X}\times\mathbb{L}\to\mathbb{L}$, a finite subset $\mathbf{X}$ of $\mathbb{X}\times\mathbb{L}$ is a labeled RFS if and only if $\mathbf{X}$ and its label set $\mathcal{L}_{\mathbf{X}}=\{\mathcal{L}(x,\ell)\}_{(x,\ell)\in\mathbf{X}}$, where $\mathcal{L}(x,\ell)=\ell$, have equal cardinality [16]. We denote compactly the distinct label indicator introduced in [16] to ensure the uniqueness of the labels in a labeled RFS as $\Delta_{\mathbf{X}}=\delta_{|\mathbf{X}|}^{(|\mathcal{L}_{\mathbf{X}}|)}$, where $|\cdot|$ represents the cardinality of a set.

An important class of the labeled RFS is the δ-GLMB RFS [16], whose distribution is

$$\boldsymbol{\pi}(\mathbf{X})=\Delta_{\mathbf{X}}\sum_{(I,\xi)\in\mathcal{F}(\mathbb{L})\times\Xi}\omega^{(I,\xi)}\delta_I^{(\mathcal{L}_{\mathbf{X}})}[p^{(\xi)}]^{\mathbf{X}} \tag{1}$$

where $\mathcal{F}(\mathbb{L})$ is the collection of all finite subsets of label space $\mathbb{L}$, and Ξ is a discrete index space, and density $p^{(\xi)}(x,\ell)$ and weight $\omega^{(I,\xi)}$ are such that $\int_{\mathbb{X}}p^{(\xi)}(x,\ell)=1$ and $\sum_{(I,\xi)\in\mathcal{F}(\mathbb{L})\times\Xi}\omega^{(I,\xi)}=1$. In multitarget tracking, each (I,ξ) represents a hypothesis that there are $|I|$ targets, whose labels are I, and that their states are determined by association map history ξ; $\omega^{(I,\xi)}$ denotes the probability that (I,ξ) is the true one, and $p^{(\xi)}(x,\ell)$ is the probability density of the kinematic state of track ℓ [16].

Another frequently used labeled RFS is the labeled multi-Bernoulli (LMB) RFS [20], whose density is

$$\boldsymbol{\pi}(\mathbf{X})=\Delta_{\mathbf{X}}\omega(\mathcal{L}_{\mathbf{X}})[p]^{\mathbf{X}} \tag{2}$$

where the weight and probability density satisfy

$$\omega(L)=\prod_{\ell\in\mathbb{L}}(1-r^{(\ell)})\prod_{\ell'\in L}\frac{1_L^{(\ell')}r^{(\ell')}}{1-r^{(\ell')}} \tag{3}$$

$$p(x,\ell)=p^{(\ell)}(x) \tag{4}$$

Given multitarget state $\mathbf{X}$, each single-target state $(x,\ell)\in\mathbf{X}$ is either detected with probability $p_D(x,\ell)$ and generates a single-target measurement z with likelihood $g(z|x,\ell)$, or missed with probability $q_D(x,\ell)=1-p_D(x,\ell)$. The multitarget measurement $Z=\{z_1,\ldots,z_M\}$ is the union of detected single-target measurements and clutter (assumed Poisson with intensity κ). Under the assumption that detections are independent conditioned on multitarget state and clutter is independent of detections, it was shown [16], [17] that the multitarget likelihood is

$$g(Z|\mathbf{X})=\lambda_Z\sum_{\theta\in\Theta(\mathcal{L}_{\mathbf{X}})}[\psi_Z^{(\theta)}]^{\mathbf{X}} \tag{5}$$

where

$$\lambda_Z=e^{-\langle\kappa,1\rangle}\kappa^Z \tag{6}$$

$$\psi_Z^{(\theta(\ell))}(x,\ell)=\begin{cases}\dfrac{p_D(x,\ell)g(z_{\theta(\ell)}|x,\ell)}{\kappa(z_{\theta(\ell)})}, & \text{if }\theta(\ell)>0\\ 1-p_D(x,\ell), & \text{if }\theta(\ell)=0\end{cases} \tag{7}$$

with θ being the association map given in [17] that described the mapping between labels in $\mathcal{L}_{\mathbf{X}}$ and the measurements in Z.

Given multitarget state $\mathbf{X}$ at time step k, each single-target state $(x,\ell)\in\mathbf{X}$ either continues to exist at time step $k+1$ with probability $p_S(x,\ell)$ and evolves to state (x_+,ℓ_+) with probability density $\delta_\ell^{(\ell_+)}f(x_+|x,\ell)$, or dies with probability $q_S(x,\ell)=1-p_S(x,\ell)$. Let the newborn multitarget state at time step $k+1$ be denoted as $\mathbf{B}_+$, then its density is [16]

$$\mathbf{f}_B(\mathbf{B}_+)=\Delta_{\mathbf{B}_+}\omega_{\mathbb{B}_+}^{(\mathcal{L}_{\mathbf{B}_+})}[p_B]^{\mathbf{B}_+} \tag{8}$$

where $\omega_{\mathbb{B}_+}^{(\mathcal{L}_{\mathbf{B}_+})}$ is the newborn weight, and $\mathbb{B}_+$ denotes the newborn label space, and p_B is the probability density of the kinematic state for newborn state at time step $k+1$. The multitarget state $\mathbf{X}_+$ is the superposition of the surviving state $\mathbf{S}_+$ and newborn state $\mathbf{B}_+$. Assuming births are independent of survivals and states evolve independently yield the multitarget transition kernel [17] in following form

$$\mathbf{f}(\mathbf{X}_+|\mathbf{X})=\mathbf{f}_S(\mathbf{X}_+\cap\mathbb{X}\times\mathbb{L}|\mathbf{X})\mathbf{f}_B(\mathbf{X}_+-\mathbb{X}\times\mathbb{L}) \tag{9}$$

where

$$\mathbf{f}_S(\mathbf{S}_+|\mathbf{X})=\Delta_{\mathbf{S}_+}\Delta_{\mathbf{X}}1_{\mathcal{L}_{\mathbf{X}}}^{(\mathcal{L}_{\mathbf{S}_+})}[\Phi_{\mathbf{S}_+}]^{\mathbf{X}} \tag{10}$$

$$\begin{aligned}\Phi_{\mathbf{S}_+}(x,\ell)=&\sum_{(x_+,\ell_+)\in\mathbf{S}_+}\delta_\ell^{(\ell_+)}p_S(x,\ell)f(x_+|x,\ell)\\&+(1-1_{\mathcal{L}_{\mathbf{S}_+}}^{(\ell)})q_S(x,\ell)\end{aligned} \tag{11}$$

To facilitate the analytic derivation of the proposed smoother, we use the following equivalent form of (9)

$$\mathbf{f}(\mathbf{X}_+|\mathbf{X})=\Delta_{\mathbf{X}_+}\Delta_{\mathbf{X}}\omega_{\mathcal{L}_{\mathbf{X}}}^{(\mathcal{L}_{\mathbf{X}_+})}[q_S]^{\mathbf{X}}[\Lambda_{\mathbf{X}}]^{\mathbf{X}_+} \tag{12}$$

$$\begin{aligned}\Lambda_{\mathbf{X}}(x_+,\ell_+)=&\sum_{(x,\ell)\in\mathbf{X}}\delta_\ell^{(\ell_+)}\rho(x,\ell)f(x_+|x,\ell)\\&+(1-1_{\mathcal{L}_{\mathbf{X}}}^{(\ell_+)})p_B(x_+,\ell_+)\end{aligned} \tag{13}$$

where the weight $\omega_{\mathcal{L}_{\mathbf{X}}}^{(L_+)} = 1_{\mathcal{L}_{\mathbf{X}}}^{(S_+)}\omega_{\mathbb{B}_+}^{(B_+)}$, with the surviving label set $S_+ = L_+ \cap \mathbb{L}$ and the new born label set $B_+ = L_+ \cap \mathbb{B}_+$, and the ratio $\rho_S(x,\ell) = p_S(x,\ell)/q_S(x,\ell)$.

Using the Bayes predict and update recursions, it was shown [16] that the δ-GLMB density is closed under the multitarget measurement likelihood (5) and multitarget transition kernel (9), which means that if the initial multitarget filtering density is δ-GLMB distributed, then the multitarget filtering densities at all subsequent times are also δ-GLMB distributed. In the following section, we show that if the multitarget filtering density is δ-GLMB distributed, then the one time step lagged multitarget smoothing density is also δ-GLMB distributed.

III. MULTITARGET TRACKING SMOOTHER

In this section, we first present a formula facilitating the derivation of the proposed smoothing algorithm, and then derive the multitarget pseudo measurement likelihood, which is the key for the closed-form derivation of the proposed smoother, and in the end, we present the analytic form of the proposed smoother.

A. ONE TIME STEP LAGGED MULTITARGET SMOOTHING

Let $\mathbf{X} = \{(x_1,\ell_1),\ldots,(x_N,\ell_N)\}$ denote the multitarget state at time step k, $\mathbf{X}_+ = \{(x_{+,1},\ell_{+,1}),\ldots,(x_{+,T_+},\ell_{+,T_+})\}$ denote the multitarget state at time step $k+1$, and $Z_+ = \{z_{+,1},\ldots,z_{+,M_+}\}$ denote the multitarget measurement at time step $k+1$. Following [28], [36], we express the one time step lagged multitarget smoothing density as

$$\boldsymbol{\pi}(\mathbf{X}|Z_+) = \boldsymbol{\pi}(\mathbf{X})\int \mathbf{f}(\mathbf{X}_+|\mathbf{X})\frac{\boldsymbol{\pi}(\mathbf{X}_+|Z_+)}{\boldsymbol{\pi}_+(\mathbf{X}_+)}\delta\mathbf{X}_+ \tag{14}$$

where $\boldsymbol{\pi}(\mathbf{X})$ represents the multitarget filtering density at time step k, $\boldsymbol{\pi}(\mathbf{X}_+|Z_+)$ and $\boldsymbol{\pi}_+(\mathbf{X}_+)$ denote the multitarget filtering and prediction densities at time step $k+1$, respectively, and $\mathbf{f}(\mathbf{X}_+|\mathbf{X})$ is the multitarget transition kernel, and the integral in (14) is the set integral introduced in [16].

According to the update of the Bayes multitarget filter [17], the multitarget filtering density at time step $k+1$ is

$$\boldsymbol{\pi}(\mathbf{X}_+|Z_+) = \frac{g(Z_+|\mathbf{X}_+)\boldsymbol{\pi}_+(\mathbf{X}_+)}{\int g(Z_+|\mathbf{X}_+)\boldsymbol{\pi}_+(\mathbf{X}_+)\delta\mathbf{X}_+} \tag{15}$$

where $g(Z_+|\mathbf{X}_+)$ and $\boldsymbol{\pi}_+(\mathbf{X}_+)$ denotes the multitarget measurement likelihood and prediction density at time step $k+1$, respectively.

Substitution of $\boldsymbol{\pi}(\mathbf{X}_+|Z_+)$ in (14) by (15) leads to the multitarget smoothing density in form of

$$\boldsymbol{\pi}(\mathbf{X}|Z_+) = \frac{\boldsymbol{\pi}(\mathbf{X})\int g(Z_+|\mathbf{X}_+)\mathbf{f}(\mathbf{X}_+|\mathbf{X})\delta\mathbf{X}_+}{\int g(Z_+|\mathbf{X}_+)\boldsymbol{\pi}_+(\mathbf{X}_+)\delta\mathbf{X}_+} \tag{16}$$

According to prediction step of the Bayes multitarget filter [17], the multitarget prediction density is

$$\boldsymbol{\pi}_+(\mathbf{X}_+) = \int \mathbf{f}(\mathbf{X}_+|\mathbf{X})\boldsymbol{\pi}(\mathbf{X})\delta\mathbf{X} \tag{17}$$

Substituting the prediction density $\boldsymbol{\pi}_+(\mathbf{X}_+)$ in (16) by (17) yields the following multitarget smoothing density

$$\boldsymbol{\pi}(\mathbf{X}|Z_+) = \frac{g(Z_+|\mathbf{X})\boldsymbol{\pi}(\mathbf{X})}{\int g(Z_+|\mathbf{X})\boldsymbol{\pi}(\mathbf{X})\delta\mathbf{X}} \tag{18}$$

where

$$g(Z_+|\mathbf{X}) = \int g(Z_+|\mathbf{X}_+)\mathbf{f}(\mathbf{X}_+|\mathbf{X})\delta\mathbf{X}_+ \tag{19}$$

From (18), we observe that the one time step lagged multitarget smoothing density $\boldsymbol{\pi}(\mathbf{X}|Z_+)$ can be acquired via the multiplication of $g(Z_+|\mathbf{X})$, which we call it the multitarget pseudo measurement likelihood in the sequel, and the multitarget filtering density $\boldsymbol{\pi}(\mathbf{X})$, followed by a normalization step. In the following section, by virtue of (19), we present the analytic form of $g(Z_+|\mathbf{X})$, which is the key for the derivation of the smoothing density in (18).

B. MULTITARGET PSEDUO MEASUREMENT LIKELIHOOD

Proposition 1: Under the multitarget measurement likelihood (5) and transition kernel (12), the multitarget pseudo measurement likelihood can be expressed as

$$\begin{aligned} &g(Z_+|\mathbf{X}) \\ &= \Delta_{\mathbf{X}}\lambda_{Z_+}\sum_{B_+\subseteq\mathbb{B}_+}\sum_{S_+\subseteq\mathcal{L}_{\mathbf{X}}}\sum_{\theta_+\in\Theta_+}\omega_{\mathbb{B}_+}^{(B_+)}[\phi_{Z_+}^{(\theta_+)}]^{B_+}[\varphi_{Z_+}^{(S_+,\theta_+)}]^{\mathbf{X}} \end{aligned} \tag{20}$$

where $\lambda_{Z_+} = e^{-\langle\kappa,1\rangle}\kappa^{Z_+}$, with κ denotes the clutter intensity; B_+ and S_+ denote respectively the surviving and newborn labels at time step $k+1$, and $\mathbb{B}_+$ denotes the newborn label space, and $\mathcal{L}_{\mathbf{X}}$ denotes the labels of multitarget state $\mathbf{X}$; and θ_+ is the association map [17] describing the mapping between labels in $S_+ \cup B_+$ and measurements in Z_+, and $\omega_{\mathbb{B}_+}^{(B_+)}$ is the newborn weight, and the base functions in (20) are

$$\phi_{Z_+}^{(\theta_+(\ell_+))}(\ell_+) = \int_{\mathbb{X}}\psi_{Z_+}^{(\theta_+(\ell_+))}(x_+,\ell_+)p_B(x_+,\ell_+)dx_+ \tag{21}$$

$$\begin{aligned} \varphi_{Z_+}^{(S_+,\theta_+(\ell))}(x,\ell) &= (1-1_{S_+}^{(\ell)})q_S(x,\ell) + 1_{S_+}^{(\ell)}p_S(x,\ell) \\ &\quad\times\int_{\mathbb{X}}\psi_{Z_+}^{(\theta_+(\ell))}(x_+,\ell)f(x_+|x,\ell)dx_+ \end{aligned} \tag{22}$$

in which $\psi_{Z_+}^{(\theta_+(\ell))}(x_+,\ell)$ denotes the single-target "likelihood" given in (7), and $p_B(x_+,\ell_+)$ is the probability density for newborn state (x_+,ℓ_+), and $q_S(x,\ell) = 1-p_S(x,\ell)$, with $p_S(x,\ell)$ denoting the survival probability, and $f(x_+|x,\ell)$ is the single-target transition density.

Proof: Substituting the analytic forms of the multitarget transition kernel $\mathbf{f}(\mathbf{X}_+|\mathbf{X})$ in (12) and the multitarget measurement likelihood $g(Z_+|\mathbf{X}_+)$ in (5) into (19) yields

$$\begin{aligned} &g(Z_+|\mathbf{X}) \\ &= \int g(Z_+|\mathbf{X}_+)\mathbf{f}(\mathbf{X}_+|\mathbf{X})\delta\mathbf{X}_+ \\ &= \int \lambda_{Z_+}\sum_{\theta_+}[\psi_{Z_+}^{(\theta_+)}]^{\mathbf{X}_+}\Delta_{\mathbf{X}_+}\Delta_{\mathbf{X}}\omega_{\mathcal{L}_{\mathbf{X}}}^{(\mathcal{L}_{\mathbf{X}_+})}[q_S]^{\mathbf{X}}[\Lambda_{\mathbf{X}}]^{\mathbf{X}_+}\delta\mathbf{X}_+ \end{aligned}$$

$$= \Delta_{\mathbf{X}}\lambda_{Z_+}[q_S]^{\mathbf{X}} \int \Delta_{\mathbf{X}_+}\omega_{\mathcal{L}_{\mathbf{X}}}^{(\mathcal{L}_{\mathbf{X}_+})} \sum_{\theta_+}[\psi_{Z_+}^{(\theta_+)}\Lambda_{\mathbf{X}}]^{\mathbf{X}_+}\delta\mathbf{X}_+$$

$$= \Delta_{\mathbf{X}}\lambda_{Z_+}[q_S]^{\mathbf{X}} \sum_{L_+}\sum_{\theta_+}\omega_{\mathcal{L}_{\mathbf{X}}}^{(L_+)}$$

$$\times[\int_{\mathbb{X}} \psi_{Z_+}^{(\theta_+(\cdot))}(x_+,\cdot)\Lambda_{\mathbf{X}}(x_+,\cdot)dx_+]^{L_+}$$

$$= \Delta_{\mathbf{X}}\lambda_{Z_+} \sum_{B_+}\sum_{S_+}\sum_{\theta_+} 1_{\mathcal{L}_{\mathbf{X}}}^{(S_+)}\omega_{\mathbb{B}_+}^{(B_+)}[\phi_{Z_+}^{(\theta_+)}]^{B_+}[\varphi_{Z_+}^{(S_+,\theta_+)}]^{\mathbf{X}} \quad (23)$$

with $\phi_{Z_+}^{(\theta_+)}$ and $\varphi_{Z_+}^{(S_+,\theta_+)}$ given by (21) and (22), respectively, and the second line from the bottom of (23) results from applying lemma 3 in [16] to the set integral in the third line from the bottom, and the last line originates from substituting $\psi_{Z_+}^{(\theta_+)}$ in (7) and $\Lambda_{\mathbf{X}}$ in (13) into the second line from the bottom.

Note that in the last line of (23), the inclusion function $1_{\mathcal{L}_{\mathbf{X}}}^{(S_+)}$ indicates that we consider the surviving label set $S_+ \subseteq \mathcal{L}_{\mathbf{X}}$ only (otherwise $1_{\mathcal{L}_{\mathbf{X}}}^{(S_+)} = 0$), and the newborn weight $\omega_{\mathbb{B}_+}^{(B_+)}$ indicates we consider the newborn label set $B_+ \subseteq \mathbb{B}_+$ only (otherwise $\omega_{\mathbb{B}_+}^{(B_+)} = 0$). Such relationships are explicitly shown in (20), and the set Θ_+ in (20) denotes the collection of the association maps whose mappings are between labels in $S_+ \cup B_+$ and the measurements in multitarget measurement Z_+.

C. ONE TIME STEP LAGGED DELTA-GENERALIZED LABELED MULTI-BERNOULLI SMOOTHING

Proposition 2: If the multitarget filtering density at time step δ-GLMB distributed in following form

$$\boldsymbol{\pi}(\mathbf{X}) = \Delta_{\mathbf{X}}\sum_{(I,\xi)}\omega^{(I,\xi)}\delta_I^{(\mathcal{L}_{\mathbf{X}})}[p^{(\xi)}]^{\mathbf{X}} \quad (24)$$

then the one time step lagged multitarget smoothing density at time step k is also δ-GLMB distributed in form of

$$\boldsymbol{\pi}(\mathbf{X}|Z_+) = \Delta_{\mathbf{X}}\sum_{(I,\xi)}\sum_{B_+\subseteq\mathbb{B}_+}\sum_{S_+\subseteq I}\sum_{\theta_+\in\Theta_+}\omega_{Z_+}^{(I,\xi,B_+,S_+,\theta_+)} \times\delta_I^{(\mathcal{L}_{\mathbf{X}})}[p^{(\xi,S_+,\theta_+)}]^{\mathbf{X}} \quad (25)$$

$$\omega^{(I,\xi,B_+,S_+,\theta_+)} \propto \omega^{(I,\xi)}\omega_{\mathbb{B}_+}^{(B_+)}[\phi_{Z_+}^{(\theta_+)}]^{B_+}[\eta_{Z_+}^{(\xi,S_+,\theta_+)}]^I \quad (26)$$

$$\eta_{Z_+}^{(\xi,S_+,\theta_+(\ell))}(\ell) = \int_{\mathbb{X}}\varphi_{Z_+}^{(S_+,\theta_+(\ell))}(x,\ell)p^{(\xi)}(x,\ell)dx \quad (27)$$

$$p^{(\xi,S_+,\theta_+(\ell))}(x,\ell) = \frac{\varphi_{Z_+}^{(S_+,\theta_+(\ell))}(x,\ell)p^{(\xi)}(x,\ell)}{\eta_{Z_+}^{(\xi,S_+,\theta_+(\ell))}(\ell)} \quad (28)$$

with $\phi_{Z_+}^{(\theta_+)}$ and $\varphi_{Z_+}^{(S_+,\theta_+)}$ given by (21) and (22), respectively.

Each (I,ξ,B_+,S_+,θ_+) represents a smoothing hypothesis that targets I with association map history ξ at time step k survive to $k+1$ with targets S_+ left, and new targets B_+ also appear at $k+1$, and the association between $S_+ \cup B_+$ and measurements in Z_+ is given by association map θ_+.

The smoothing weight $\omega^{(I,\xi,B_+,S_+,\theta_+)}$ is proportional to filtering weight $\omega^{(I,\xi)}$ scaled by $\omega_{\mathbb{B}_+}^{(B_+)}[\phi_{Z_+}^{(\theta_+)}]^{B_+}[\eta_{Z_+}^{(\xi,S_+,\theta_+)}]^I$, and the single-target smoothing density $p^{(\xi,S_+,\theta_+(\ell))}(x,\ell)$ is obtained by using the single-target filtering density $p^{(\xi)}(x,\ell)$ and the function $\varphi_{Z_+}^{(S_+,\theta_+(\ell))}(x,\ell)$ via the Bayes rule. Note that we can omit the S_+ and B_+ in (25) since they are implicitly encapsulated in association map θ_+, thus (25) is indeed a δ-GLMB, and the proposed smoother is capable of generating target tracks directly.

Proof: Using (20) and (24), we calculate the numerator of (18) as

$$g(Z_+|\mathbf{X})\boldsymbol{\pi}(\mathbf{X}) = \lambda_{Z_+}\Delta_{\mathbf{X}}\sum_{(I,\xi)}\sum_{B_+\subseteq\mathbb{B}_+}\sum_{S_+\subseteq\mathcal{L}_{\mathbf{X}}}\sum_{\theta_+\in\Theta_+}\omega^{(I,\xi)} \times\omega_B^{(B_+)}[\phi_{Z_+}^{(\theta_+)}]^{B_+}\delta_I^{(\mathcal{L}_{\mathbf{X}})}[p^{(\xi)}\varphi_{Z_+}^{(S_+,\theta_+)}]^{\mathbf{X}}$$

$$= \lambda_{Z_+}\Delta_{\mathbf{X}}\sum_{(I,\xi)}\sum_{B_+\subseteq\mathbb{B}_+}\sum_{S_+\subseteq I}\sum_{\theta_+\in\Theta_+}\omega^{(I,\xi)} \times\omega_B^{(B_+)}[\phi_{Z_+}^{(\theta_+)}]^{B_+}\delta_I^{(\mathcal{L}_{\mathbf{X}})}[\eta_{Z_+}^{(\xi,S_+,\theta_+)}]^{\mathcal{L}_{\mathbf{X}}}[p^{(\xi,S_+,\theta_+)}]^{\mathbf{X}} \quad (29)$$

where the last line results from the following identity

$$p^{(\xi,S_+,\theta_+(\ell))}(x,\ell)\eta_{Z_+}^{(\xi,S_+,\theta_+(\ell))}(\ell) = p^{(\xi)}(x,\ell)\varphi_{Z_+}^{(S_+,\theta_+(\ell))}(x,\ell) \quad (30)$$

Using (29), the denominator of (18) becomes

$$\int g(Z_+|\mathbf{X})\boldsymbol{\pi}(\mathbf{X})\delta\mathbf{X}$$

$$= \lambda_{Z_+}\sum_{(I,\xi)}\sum_{B_+\subseteq\mathbb{B}_+}\sum_{S_+\subseteq I}\sum_{\theta_+\in\Theta_+}\omega^{(I,\xi)}\omega_{\mathbb{B}_+}^{(B_+)}[\phi_{Z_+}^{(\theta_+)}]^{B_+} \times\int\Delta_{\mathbf{X}}\delta_I^{(\mathcal{L}_{\mathbf{X}})}[\eta_{Z_+}^{(\xi,S_+,\theta_+)}]^{\mathcal{L}_{\mathbf{X}}}[p^{(\xi,S_+,\theta_+)}]^{\mathbf{X}}\delta\mathbf{X}$$

$$= \lambda_{Z_+}\sum_{(I,\xi)}\sum_{B_+\subseteq\mathbb{B}_+}\sum_{S_+\subseteq I}\sum_{\theta_+\in\Theta_+}\omega^{(I,\xi)} \times\omega_{\mathbb{B}_+}^{(B_+)}[\phi_{Z_+}^{(\theta_+)}]^{B_+}[\eta_{Z_+}^{(\xi,S_+,\theta_+)}]^I \quad (31)$$

where the last line of (31) follows directly from lemma 3 in [16]. Substitutions of (29) and (31) into (18) leads to (25).

IV. IMPLEMENTATION

In this section, we present an efficient implementation of the proposed smoothing algorithm by truncating the multitarget smoothing density without enumeration of all the smoothing hypotheses and calculating their corresponding weights via the standard ranked assignment algorithm.

A. TRUNCATION OF SMOOTHING DENSITY

According to proposition 2, each filtering hypothesis (I,ξ) generates a new set of smoothing hypotheses (I,ξ,B_+,S_+,θ_+), with the newborn label set $B_+ \subseteq \mathbb{B}_+$, surviving label set $S_+ \subseteq I$, and association map $\theta_+ \in \Theta_+(S_+ \cup B_+)$.

For a given label set I, since $S_+ \subseteq I$, thus there are $2^{|I|}$ possibilities of S_+, where $|\cdot|$ represents the cardinality of a set; similarly, given newborn label space $\mathbb{B}_+$, since $B_+ \subseteq \mathbb{B}_+$, thus we have $2^{|\mathbb{B}_+|}$ possibilities of B_+. There are $2^{|\mathbb{B}_+|+|I|}$ possibilities of pair (B_+, S_+), therefore there are $\sum_{u=1}^{2^{|\mathbb{B}_+|+|I|}} |\Theta_+(B_+^{(u)} \cup S_+^{(u)})|$ possibilities of triplet (B_+, S_+, θ_+), where $(B_+^{(u)}, S_+^{(u)})$ represents the u th pair of (B_+, S_+), and $\Theta_+(B_+^{(u)}, S_+^{(u)})$ denotes the collection of the association maps between label set $B_+^{(u)} \cup S_+^{(u)}$ and multitarget measurement Z_+. Due to the large number of the smoothing hypotheses, thus it is generally intractable to keep all the smoothing hypotheses at each time step. Therefore, we choose to truncate the smoothing density by keeping only the components with significant weights

$$\boldsymbol{\pi}(\mathbf{X}|Z_+) = \Delta_{\mathbf{X}} \sum_{(I,\xi)} \sum_{(B_+,S_+,\theta_+)\in\Gamma(I,\xi)} \omega_{Z_+}^{(I,\xi,B_+,S_+,\theta_+)} \times \delta_I^{(\mathcal{L}\mathbf{x})}[p^{(\xi,S_+,\theta_+)}]^{\mathbf{X}} \tag{32}$$

where for a given (I,ξ), $\Gamma(I,\xi) = \{(B_+^{(m)}, S_+^{(m)}, \theta_+^{(m)})\}_{m=1}^{M^{(I,\xi)}}$ is the set of the $M^{(I,\xi)}$ elements whose weights $\omega_{Z_+}^{(I,\xi,B_+^{(m)},S_+^{(m)},\theta_+^{(m)})}$ are the highest, and $\omega_{Z_+}^{(I,\xi,B_+,S_+,\theta_+)}$ is the renormalized weight after truncation. It is clear that the number of kept smoothing hypotheses $M^{(I,\xi)}$ is a filtering hypothesis (I,ξ) dependent parameter, and in this work, $M^{(I,\xi)}$ is chosen to be proportional to its filtering weight $\omega^{(I,\xi)}$, i.e., $M^{(I,\xi)} = [M\omega^{(I,\xi)}]$, where M is the predetermined number of the overall smoothing hypotheses, and $[\cdot]$ represents the operation of rounding towards its nearest integer.

As shown above, it is infeasible, especially in cases where the target number is large, to list all the possible smoothing hypotheses, calculate their weights, and then choose those with the highest weights. Nonetheless, we show that if the newborn multitarget state follows a LMB process, then the truncation of the smoothing density in (32) can be solved efficiently via the ranked assignment technique.

B. RANKED ASSIGNMENT FORMULATION

According to (26), the weight of smoothing hypothesis (I,ξ,B_+,S_+,θ_+) is

$$\omega^{(I,\xi,B_+,S_+,\theta_+)} \propto \omega^{(I,\xi)}\omega_{\mathbb{B}_+}^{(B_+)}[\phi_{Z_+}^{(\theta_+)}]^{B_+}[\eta_{Z_+}^{(\xi,S_+,\theta_+)}]^I \tag{33}$$

Since we assume the births is an LMB process, then using (3), we rewrite the newborn weight $\omega_{\mathbb{B}_+}^{(B_+)}$ as

$$\omega_{\mathbb{B}_+}^{(B_+)} = [r_B]^{B_+}[1-r_B]^{\mathbb{B}_+-B_+} \tag{34}$$

where the subtraction sign in $\mathbb{B}_+ - B_+$ denotes the set difference operation, and $r_B^{(\ell)}$ denotes the birth probability of label $\ell \in \mathbb{B}_+$.

Replacing $\omega_{\mathbb{B}_+}^{(B_+)}$ in (33) by (34) leads to

$$\begin{aligned}\omega^{(I,\xi,B_+,S_+,\theta_+)} &\propto \omega^{(I,\xi)}[r_B\phi_{Z_+}^{(\theta_+)}]^{B_+}[1-r_B]^{\mathbb{B}_+-B_+}[\eta_{Z_+}^{(\xi,S_+,\theta_+)}]^I \\ &= \omega^{(I,\xi)}[\gamma_{Z_+}^{(B_+,\theta_+)}]^{\mathbb{B}_+}[\eta_{Z_+}^{(\xi,S_+,\theta_+)}]^I\end{aligned} \tag{35}$$

in which

$$\gamma_{Z_+}^{(B_+,\theta_+)}(\ell) = \begin{cases} r_B^{(\ell)}\phi_{Z_+}^{(\theta_+(\ell))}(\ell), & \text{if } \ell \in B_+ \\ 1-r_B^{(\ell)}, & \text{if } \ell \in \mathbb{B}_+ - B_+ \end{cases} \tag{36}$$

For a given (I,ξ), according to (35), if we can generate (B_+,S_+,θ_+) in decreasing order of $[\gamma_{Z_+}^{(B_+,\theta_+)}]^{\mathbb{B}_+}[\eta_{Z_+}^{(\xi,S_+,\theta_+)}]^I$ efficiently, then the truncation of the smoothing density is solved. Next, we show that the generation of those triplets can be cast into a ranked assignment problem.

Let the multitarget measurement $Z_+ = \{z_{+,1},\ldots,z_{+,M_+}\}$, the newborn label space $\mathbb{B}_+ = \{\ell_1,\ldots,\ell_{|\mathbb{B}_+|}\}$, and the label set $I = \{\ell_1,\ldots,\ell_{|I|}\}$.We write the label union $L = \mathbb{B}_+ \cup I$ in form of

$$L = \{\ell_1,\ldots,\ell_{|\mathbb{B}_+|},\ell_{|\mathbb{B}_+|+1},\ldots,\ell_{|\mathbb{B}_+|+|I|}\} \tag{37}$$

in which $\ell_1,\ldots,\ell_{|\mathbb{B}_+|}$ denote the labels in $\mathbb{B}_+$, and $\ell_{|\mathbb{B}_+|+1},\ldots,\ell_{|\mathbb{B}_+|+|I|}$ denote the labels in I. It is clear that there are total $N_+ = |\mathbb{B}_+| + |I|$ labels in label set L.

Given filtering hypothesis (I,ξ), each triplet (B_+,S_+,θ_+) is equivalent to an assignment matrix $\mathbf{A}$ with $N_+ \times (M_+ + 2N_+)$ binary entries, with the row index $i \in \{1,\ldots,N_+\}$ denoting the label index of the element in L and the column index $j \in \{1,\ldots,M_+ + 2N_+\}$ denoting the measurement index.

The assignment matrix $\mathbf{A}$ consists of three parts, namely $\mathbf{A} = [\mathbf{A}_1,\mathbf{A}_2,\mathbf{A}_3]$, with the first part $\mathbf{A}_1$ accounts for association between the labels in L and the multitarget measurement $Z_+ = \{z_{+,1},\ldots,z_{+,M_+}\}$, i.e., for $i \in \{1,\ldots,N_+\}$, $j \in \{1,\ldots,M_+\}$, $\mathbf{A}_{i,j} = 1$ denotes that label ℓ_i generates measurement $z_{+,j}$; the second sub-matrix $\mathbf{A}_2$ accounts for the missed detections for labels in L, i.e., for $i \in \{1,\ldots,N_+\}$, $j = M_+ + i$, $\mathbf{A}_{i,j} = 1$ represents that label ℓ_i misses its detection; and the third sub-matrix $\mathbf{A}_3$ denotes the cases where the label ℓ_i disappears at time $k+1$, i.e., for $i \in \{1,\ldots,N_+\}$, $j = M_+ + N_+ + i$, $\mathbf{A}_{i,j} = 1$ indicates that if label $\ell_i \in I$, then it does not survive to time $k+1$ and if label $\ell_i \in \mathbb{B}_+$, then it is not born.

We construct the cost matrix accordingly as

$$\mathbf{C} = [\mathbf{C}_1,\mathbf{C}_2,\mathbf{C}_3] \tag{38}$$

with the first sub-matrix $\mathbf{C}_1$ accounting for the costs between the mapping of label set L in and the multitarget measurements Z_+ given by

$$\mathbf{C}_{i,j} = -\log \begin{cases} r_B^{(\ell_i)}\phi_{Z_+}^{(j)}(\ell_i), & \text{if } i \in \{1:N_{\mathbb{B}_+}\},\ j \in \{1:M_+\} \\ \eta_{Z_+}^{(\xi,S_+,j)}(\ell_i), & \text{if } i \in \{N_{\mathbb{B}_+}+1:N_+\},\ j \in \{1:M_+\} \end{cases} \tag{39}$$

and the second part $\mathbf{C}_2$ defining the cost when the labels in L miss their detections given by

$$\mathbf{C}_{i,j} = -\log \begin{cases} r_B^{(\ell_i)}\phi_{Z_+}^{(0)}(\ell_i), & \text{if } i \in \{1:N_{\mathbb{B}_+}\},\ j = M_+ + i \\ \eta_{Z_+}^{(\xi,S_+,\emptyset)}(\ell_i), & \text{if } i \in \{N_{\mathbb{B}_+}+1:N_+\},\ j = M_+ + i \end{cases} \tag{40}$$

and the last part $\mathbf{C}_3$ accounts for the cases when labels in newborn label space $\mathbb{B}_+$ do not appear and labels in I do not survive given by

$$\mathbf{C}_{i,j} = -\log \begin{cases} 1 - r_B^{(\ell_i)} \text{ if } i \in \{1 : N_{\mathbb{B}_+}\},\ j = M_+ + N_+ + i \\ 1 - p_S(\ell_i),\ \text{if } i \in \{N_{\mathbb{B}_+} + 1 : N_+\},\ j = M_+ + N_+ + i \end{cases} \tag{41}$$

In (39), (40) and (41), we use $\{N_1 : N_2\}$ to denote $\{N_1, \ldots, N_2\}$ for compactness. The functions $\eta_{Z_+}^{(\xi,S_+,j)}(\ell_i)$ and $\phi_{Z_+}^{(j)}(\ell_i)$ in (39) and (40) are given by (27) and (21), respectively.

Note that the costs in the non-diagonal elements of the second and third parts of $\mathbf{C}$ in (38) are set to positive infinity to prevent those assignments from happening, i.e., $\mathbf{C}_{i,j} = +\infty$, for $i \in \{1, \ldots, N_+\}$, $j \in \{M_+ + 1, \ldots, M_+ + 2N_+\}$, but $j \neq i + N_+$, $j \neq i + N_+ + M_+$, since for any label in L, it misses its detection or die only once.

Now, the overall cost for making assignment $\mathbf{A}$ is

$$c_{\mathbf{A}} = \sum_{i=1}^{N_+} \sum_{j=1}^{M_+ + 2N_+} \mathbf{C}_{i,j} \mathbf{A}_{i,j} \tag{42}$$

The key observation is that

$$[\gamma_{Z_+}^{(B_+,\theta_+)}]^{\mathbb{B}_+} [\eta_{Z_+}^{(\xi,S_+,\theta_+)}]^I = \exp(-c_{\mathbf{A}}) \tag{43}$$

which means that for a given (I, ξ), generating a new set of triplets (B_+, S_+, θ_+) with highest weights $\omega^{(I,\xi,B_+,S_+,\theta_+)}$ in decreasing order is equivalent to generating a group of assignments $\mathbf{A}$ with lowest costs $c_{\mathbf{A}}$ in increasing order. By constructing the cost matrix $\mathbf{C}$ in (38), it turns out that the truncation of the multitarget smoothing density in (32) transforms into a ranked two-dimensional assignment problem, which can be solved efficiently using the Murty's algorithm [37].

C. COMPUTE PARAMTERS

We now provide a detailed computation of the cost matrix in (38), the normalizing factor in (27) and the single-target smoothing density in (28).

To have an analytic solution, we consider linear Gaussian multitarget model [38] only, which means that the single-target transition density $f(x_+|x, \ell)$ and the measurement likelihood function $g(z|x, \ell)$ satisfy

$$f(x_+|x, \ell) = \mathcal{N}(x_+; \mathbf{F}x, \mathbf{Q}) \tag{44}$$

$$g(z|x, \ell) = \mathcal{N}(z; \mathbf{H}x, \mathbf{R}) \tag{45}$$

where $\mathcal{N}(\cdot; \mathbf{m}, \mathbf{P})$ denotes a Gaussian density with mean $\mathbf{m}$ and covariance matrix $\mathbf{P}$, and $\mathbf{F}$ is the state transition matrix, $\mathbf{Q}$ is the covariance matrix of the process noise, $\mathbf{H}$ is the measurement matrix, $\mathbf{R}$ is the covariance matrix of the measurement noise. We further assume that the survival and detection probabilities depend on label only, which means that $p_S(x, \ell) = p_S(\ell)$ and $p_D(x, \ell) = p_D(\ell)$.

Suppose that each single-target filtering density and the density of the new-born state are

$$p^{(\xi)}(x, \ell) = \sum_{n=1}^{N_\xi(\ell)} \omega_\xi^{(n)}(\ell) \mathcal{N}(x; \mathbf{m}_\xi^{(n)}(\ell), \mathbf{P}_\xi^{(n)}(\ell)) \tag{46}$$

$$p_B(x_+, \ell_+) = \sum_{n=1}^{N_B(\ell_+)} \omega_B^{(n)}(\ell_+) \mathcal{N}(x_+; \mathbf{m}_B^{(n)}(\ell_+), \mathbf{P}_B^{(n)}(\ell_+)) \tag{47}$$

then the key ingredients $\phi_{Z_+}^{(j)}(\ell_i)$ and $\eta_{Z_+}^{(\xi,S_+,j)}(\ell_i)$ in cost matrix $\mathbf{C}_{i,j}$ in (38) are given by

$$\phi_{Z_+}^{(j)}(\ell_i) = \begin{cases} \dfrac{p_D(\ell_i)\varepsilon_j(\ell_i)}{\kappa(z_{+,j})}, & \text{if } j \in \{1, \ldots, M_+\} \\ 1 - p_D(\ell_i), & \text{if } j = 0 \end{cases} \tag{48}$$

where

$$\varepsilon_j(\ell_i) = \sum_{n=1}^{N_B(\ell_i)} \omega_B^{(n)}(\ell_i) \mathcal{N}(z_{+,j}; z_B^{(n)}(\ell_i), \mathbf{S}_B^{(n)}(\ell_i)) \tag{49}$$

$$z_B^{(n)}(\ell_i) = \mathbf{H}\mathbf{m}_B^{(n)}(\ell_i) \tag{50}$$

$$\mathbf{S}_B^{(n)}(\ell_i) = \mathbf{H}\mathbf{P}_B^{(n)}(\ell_i)\mathbf{H}^T + \mathbf{R} \tag{51}$$

and

$$\eta_{Z_+}^{(\xi,S_+,j)}(\ell_i) = \begin{cases} \dfrac{p_S(\ell_i)p_D(\ell_i)\beta_j(\ell_i)}{\kappa(z_{+,j})}, & \text{if } j \in \{1, \ldots, M_+\} \\ p_S(\ell_i)(1 - p_D(\ell_i)), & \text{if } j = 0 \end{cases} \tag{52}$$

with

$$\beta_j(\ell_i) = \sum_{n=1}^{N_\xi(\ell_i)} \omega_\xi^{(n)}(\ell_i) \mathcal{N}(z_{+,j}; z_\xi^{(n)}(\ell_i), \mathbf{S}_\xi^{(n)}(\ell_i)) \tag{53}$$

$$z_\xi^{(n)}(\ell_i) = \mathbf{H}\mathbf{F}\mathbf{m}_\xi^{(n)}(\ell_i) \tag{54}$$

$$\mathbf{S}_\xi^{(n)}(\ell_i) = \mathbf{H}(\mathbf{F}\mathbf{P}_\xi^{(n)}(\ell_i)\mathbf{F}^T + \mathbf{Q})\mathbf{H}^T + \mathbf{R} \tag{55}$$

Equation (48) is acquired by substituting (7) and (47) into (21); and (52) is acquired by substituting (22) and (46) into (27), and then use the following identity [36]

$$\int \mathcal{N}(z; \mathbf{H}x', \mathbf{R})\mathcal{N}(x'; \mathbf{F}x, \mathbf{Q})dx' = \mathcal{N}(z; \mathbf{H}\mathbf{F}x, \mathbf{H}\mathbf{Q}\mathbf{H}^T + \mathbf{R})$$

Substituting (22) and (46) into (28) yields the single-target smoothing density

$$p^{(\xi,S_+,\theta_+(\ell))}(x, \ell) = \sum_{n=1}^{N_\xi(\ell)} \omega_{\xi,S_+,\theta_+}^{(n)}(\ell) \mathcal{N}(x; \mathbf{m}_{\xi,S_+,\theta_+}^{(n)}(\ell), \mathbf{P}_{\xi,S_+,\theta_+}^{(n)}(\ell)) \tag{56}$$

where

$$\omega_{\xi,S_+,\theta_+}^{(n)}(\ell) = \omega_\xi^{(n)}(\ell) q_{\xi,S_+,\theta_+}^{(n)}(\ell) / \sum_{n=1}^{N_\xi(\ell)} \omega_\xi^{(n)}(\ell) q_{\xi,S_+,\theta_+}^{(n)}(\ell) \tag{57}$$

$$q_{\xi,S_+,\theta_+}^{(n)}(\ell) = \mathcal{N}(z_{+,\theta_+(\ell)}; z_\xi^{(n)}(\ell), \mathbf{S}_\xi^{(n)}(\ell)) \tag{58}$$

TABLE 2. Pseudo code for one smoothing recursion.

Algorithm 1

Inputs: $\{(w^{(h)}, p^{(h)}), M^{(h)}\}_{h=1}^{H}$, Z_+

Outputs: $\{(w^{(h,m)}, p^{(h,m)})\}_{(h,m)=(1,1)}^{(H,M^{(h)})}$

for $h = 1 : H$ do

  Find $C^{(h)}$ using (39), (40) and (41)

  Find $\{(S_+^{(m)}, B_+^{(m)}, q_+^{(m)})\}_{m=1}^{M^{(h)}} := murty(C^{(h)}, M^{(h)})$

  for $m = 1 : M^{(h)}$ do

    Find $h_{Z_+}^{(h,m)} = h_{Z_+}^{(x,S_+^{(m)},q_+^{(m)})}$ using (27)

    Find $p^{(h,m)} = p^{(x,S_+^{(m)},q_+^{(m)})}$ using (28)

    Find $w^{(h,m)} = w^{(I,x,S_+^{(m)},B_+^{(m)},q_+^{(m)})}$ using (26)

  end

end

Normalize smoothing weights $\{w^{(h,m)}\}_{(h,m)=(1,1)}^{(H,M^{(h)})}$

$$\mathbf{m}_{\xi,S_+,\theta_+}^{(n)}(\ell) = \mathbf{m}_{\xi}^{(n)}(\ell) + \mathbf{K}_{\xi,S_+,\theta_+}^{(n)}(\ell)(z_{+,\theta_+(\ell)} - z_{\xi}^{(n)}(\ell)) \tag{59}$$

$$\mathbf{K}_{\xi,S_+,\theta_+}^{(n)}(\ell) = \mathbf{P}_{\xi}^{(n)}(\ell)\mathbf{F}^T\mathbf{H}^T\mathbf{S}_{\xi}^{(n)}(\ell)^{-1} \tag{60}$$

$$\mathbf{P}_{\xi,S_+,\theta_+}^{(n)}(\ell) = (\mathbf{I} - \mathbf{K}_{\xi,S_+,\theta_+}^{(n)}(\ell)\mathbf{HF})\mathbf{P}_{\xi}^{(n)}(\ell) \tag{61}$$

with $z_{\xi}^{(n)}(\ell)$ and $\mathbf{S}_{\xi}^{(n)}(\ell)$ in (58) given by (54) and (55), respectively.

Note that (56) holds only when $1_{S_+}^{(\ell)} = 1$ and $\theta_+(\ell) > 0$. If $1_{S_+}^{(\ell)} = 0$ or $\theta_+(\ell) = 0$, then the single-target smoothing density is identical to the filtering density

$$p^{(\xi,S_+,\theta_+(\ell))}(x, \ell) = p^{(\xi)}(x, \ell) \tag{62}$$

This is an intuitive result, since $1_{S_+}^{(\ell)} = 0$ indicates that label ℓ does not survive, and $\theta_+(\ell) = 0$ indicates it misses its detection. In both cases, since no measurement is available for smoothing, thus the single-target smoothing density should be identical to the filtering density.

A pseudo-code for one recursion of the δ-GLMB smoother is given in Table 2, in which we replace the δ-GLMB filtering density $\{(\omega^{(I,\xi)}, p^{(\xi)})\}_{(I,\xi)}$ by $\{(\omega^{(h)}, p^{(h)})\}_{h=1}^{H}$, and the number of kept smoothing hypotheses $M^{(I,\xi)}$ is also replaced by $M^{(h)}$. We denote the truncated δ-GLMB smoothing density accordingly as $\{(\omega^{(h,m)}, p^{(h,m)})\}_{(h,m)=(1,1)}^{(H,M^{(h)})}$, and the function *murty* in Table 2 refers to the Murty's algorithm [37].

V. NUMERICAL RESULTS

In this section, we show the comparison of the proposed smoother with the PHD [28], MB [30], and CPHD [31] smoothers, and then presents its comparison with the LMB [33], and δ-GLMB-A [35] smoothers, and the δ-GLMB filter, and in the end, we present an experiment result.

All smoothers used in this section share the lag of one time step, and the optimal subpattern assignment (OSPA) [39] and generalized OSPA (GOSPA) [40] are chosen as the performance metrics.

TABLE 3. Target/sensor geometry.

Target /Sensor	Initial Location (m)	Initial Velocity (m/s)	Existing Time (s)
Target 1	(600, 250)	(-10, 0)	[5,50]
Target 2	(140, 140)	(-10, 0)	[10,40]
Target 3	(-145, 150)	(10, 0)	[1,45]
Sensor	(0, 0)	(1, 0)	[1,50]

We assume that all targets and the sensor move with constant velocity on the same x-y plane. Table 3 presents the initial positions, velocities and durations of these targets and the sensor. Since our aim is to track the bearings of those targets, thus we denote the target state by $x_k = [\beta_k, \dot{\beta}_k, \ddot{\beta}_k]^T$, where β_k represents the bearing, $\dot{\beta}_k$ and $\ddot{\beta}_k$ denote its first and second order time derivatives. The temporal evolvement of state x_k is described by the discrete Wiener acceleration model [41]

$$x_{k+1} = \mathbf{F}x_k + \mathbf{\Gamma}v_k \tag{63}$$

where the processing noise $v_k \sim \mathcal{N}(0, \sigma_v^2)$, with

$$\mathbf{F} = \begin{bmatrix} 1 & \Delta & \Delta^2/2 \\ 0 & 1 & \Delta \\ 0 & 0 & 1 \end{bmatrix}, \quad \mathbf{\Gamma} = \begin{bmatrix} \Delta^2/2 \\ \Delta \\ 1 \end{bmatrix} \tag{64}$$

in which Δ is the sampling period.

Available measurement is the bearing from sensor to target, referenced (clockwise positive) to the y-axis, i.e., angle between y-axis and line of sight, and the measurement equation is

$$z_k = \mathbf{H}x_k + w_k \tag{65}$$

where the measurement matrix $\mathbf{H} = [1, 0, 0]$, and measurement noise $w_k \sim \mathcal{N}(0, \sigma_w^2)$.

In the first simulation, the simulation time is 50 s, and the sampling period is $\Delta = 1$ s, and the standard deviations of the process and measurement noises are $\sigma_v = 0.05(^\circ/s^2)$ and $\sigma_w = 1^\circ$, and for convenience, we assume the detection and survival probabilities are label independent, i.e., $p_D(\ell) = p_D$, and $p_S(\ell) = p_S$, with $p_D = 0.9$, and $p_S = 0.98$. The clutter is a Poisson process with average clutter number $\lambda_c = 4$ and a uniform spatial distribution over measurement space of $\mathbb{Z} = (-180^\circ, 180^\circ]$.

The birth process is an LMB process with parameters set $\{r_B^{(i)}, p_B^{(i)}\}_{i=1}^{3}$, where the probability of birth is $r_B^{(i)} = 0.02$, and the Gaussian densities $p_B^{(i)}(x) = \mathcal{N}(x; \mathbf{m}_B^{(i)}, \mathbf{P}_B)$ share the covariance matrix $\mathbf{P}_B = \text{diag}([4, 0.5, 0.2]^T)$, but have different means that are given by $\mathbf{m}_B^{(1)} = [67, 0, 0]^T$, $\mathbf{m}_B^{(2)} = [41, 0, 0]^T$, and $\mathbf{m}_B^{(3)} = [-42, 0, 0]^T$.

A. SIMULATION 1

Fig. 1 shows a sample run of the proposed δ-GLMB smoother. The input, which are cluttered and noisy bearing measurements, are shown in Fig. 1(a), and the output, which are

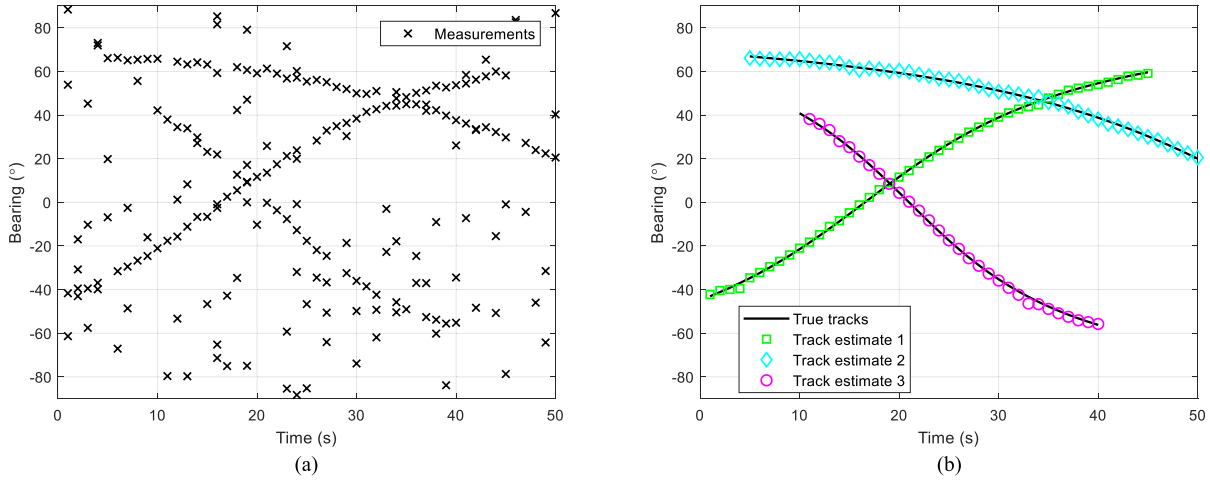

FIGURE 1. A sample run of the proposed smoother for simulation 1. (a) Input (measurements), (b) Output (Track estimates).

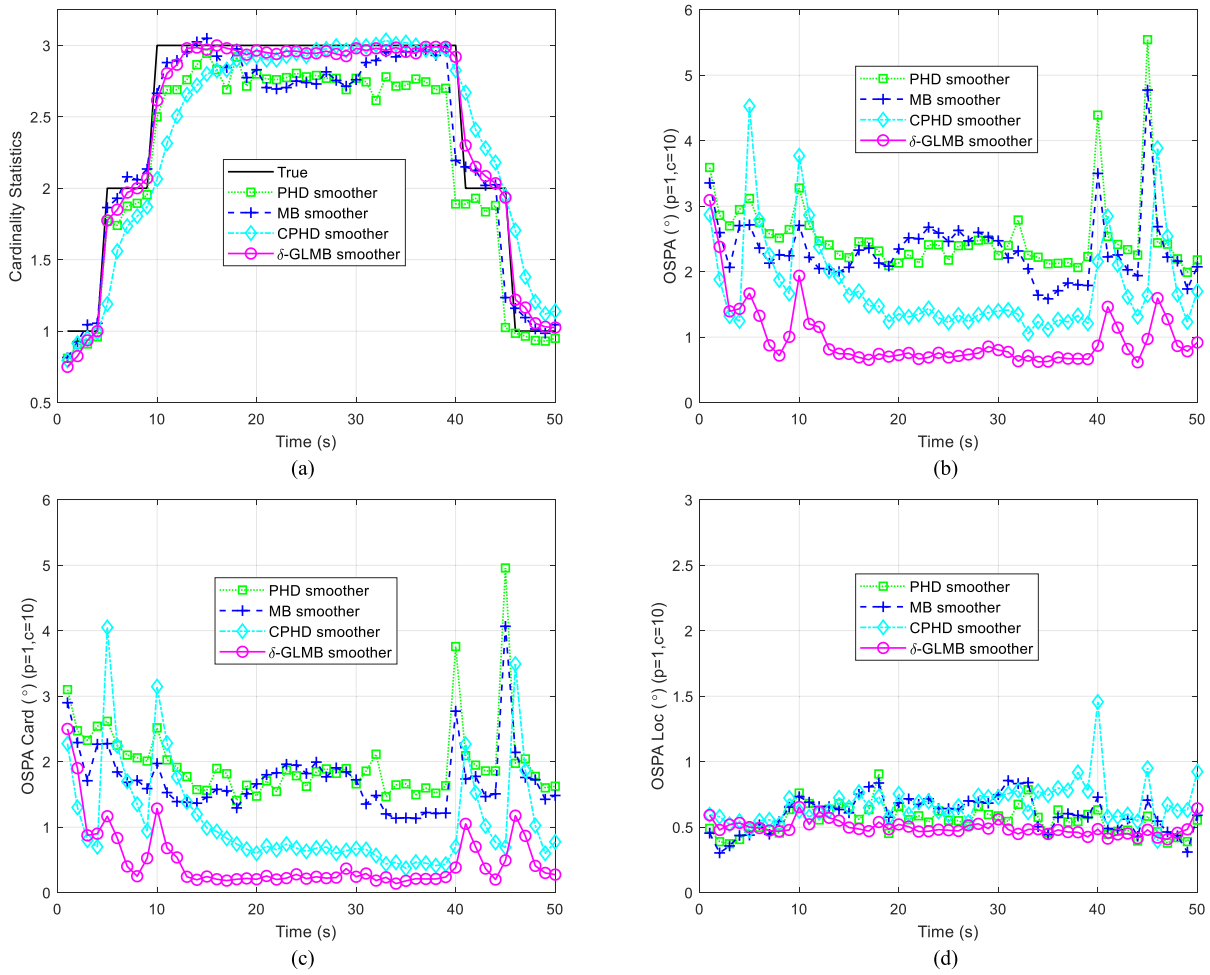

FIGURE 2. Cardinality statistic and OSPA distance for simulation 1 (200 MC runs). (a) Cardinality statistic, (b) OSPA distance, (c) OSPA cardinality error, (d) OSPA localization error.

labeled track estimates, are presented in Fig. 1(b). Each unique track color in Fig. 1(b) originates form a unique label. In this run, we observe that the proposed smoother produces accurate estimates of target number and state, except for a small delay of initiating one track.

Fig. 2 reports the cardinality statistic and OSPA distance of the PHD [28], MB [30], CPHD [31] and the δ-GLMB smoothers over 200 Monte Carlo runs. Figs. 2(a) and (b) reveal that the δ-GLMB smoother outperforms the PHD, MB, and CPHD smoothers with the lag of one time step.

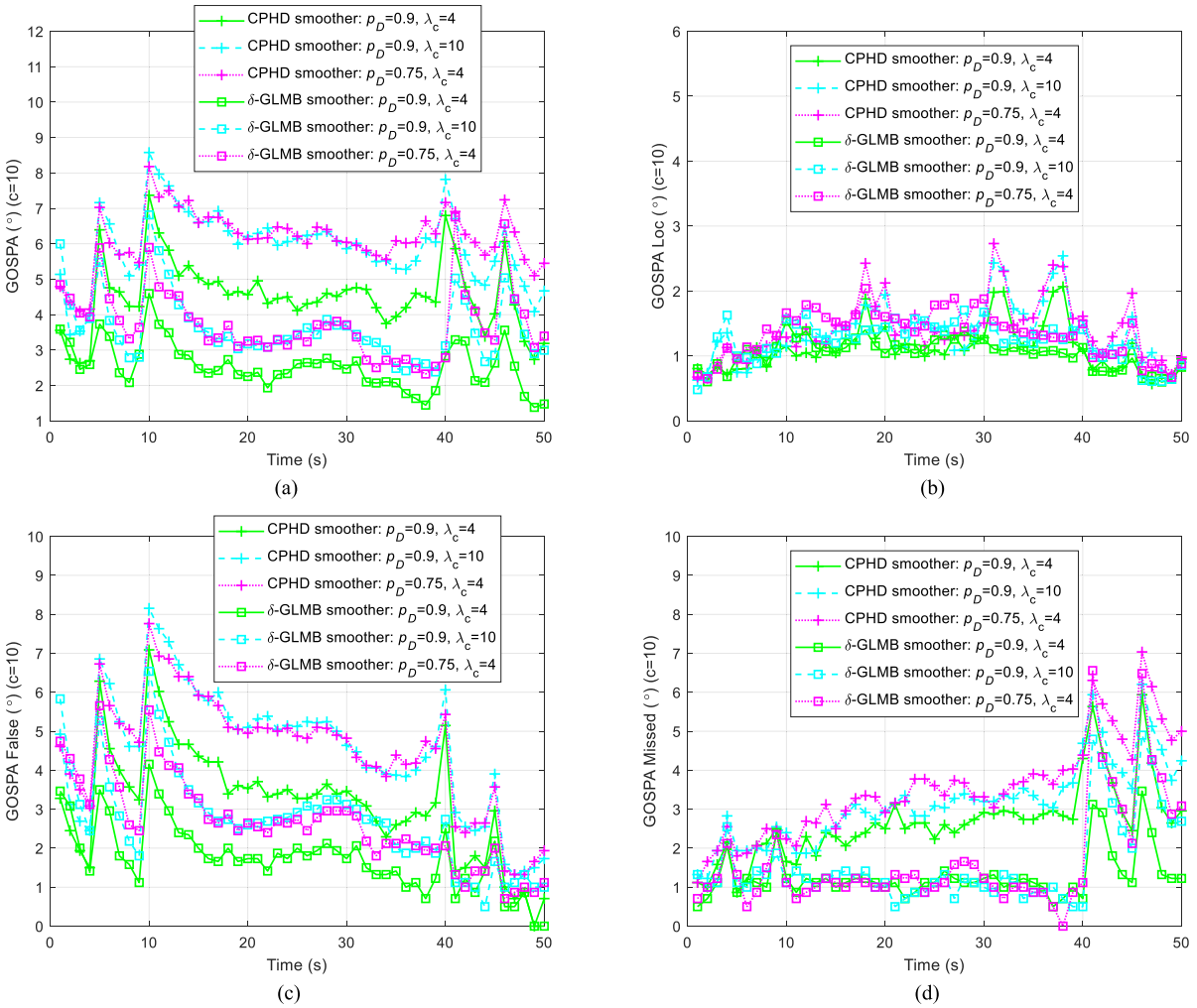

FIGURE 3. **Mean GOSPA error for simulation 1 (200 MC runs). (a) GOSPA, (b) GOSPA localization error (c) GOSPA false error (d) GOSPA missed error.**

In specific, we observe from Figs. 2(c) and (d) that the δ-GLMB smoother outperforms other three one time step lagged smoothers in terms of both the OSPA cardinality and localization errors.

Fig. 2(a) reveals that the cardinality estimates of the δ-GLMB and CPHD smoothers are far better than those of the PHD and MB smoothers, which severely underestimate the target number. Compared to the CPHD smoother, the cardinality estimates of the δ-GLMB smoother are closer to the truth. In the average sense, the response of the δ-GLMB smoother to target birth is faster than that of the CPHD smoother, whereas its response to target death is slightly quicker than that of the CPHD smoother. The prompt response of the δ-GLMB smoother attributes mainly to the fast response of the δ-GLMB filter [34] to target birth or death because the smoothing density relies on both the filtering density and the measurements indicating the true target number. The PHD and MB smoothers suffer from the premature target death [23], [25] at 40s, 45s, which are also seen by the large OSPA cardinality errors at those moments in Fig. 2(c).

Besides, we also observe that the OSPA localization errors of the CPHD smoother at target death times, for example at 40s, 45s, are significant larger than those at other times. A potential reason is that the CPHD smoother suffers from the 'spooky effect' [17], [42]. The deaths of targets at 41s, 46s can be viewed as misdetections, which lead to the PHD of the CPHD smoothing density shifting to the states of existing targets, thus the PHD at the state of the disappeared target would become relatively low. According to Fig. 2(a), it is highly likely the number of targets given by the CPHD smoother is identical to the true cardinality. This leads to the situation where there are two estimates around one of the states of the existing targets, while around the true state of the disappeared target, there are no estimates, which eventually lead to the large OSPA localization errors at those moments.

We tested the δ-GLMB smoother on two more difficult scenarios in terms of the more recently proposed GOSPA metric [40], which allows us to penalize localization errors for detected targets and the errors due to missed and false targets.

TABLE 4. Root mean square gospa errors for simulation 1.

Setting	$p_D = 0.9$, $\lambda_c = 4$		$p_D = 0.9$, $\lambda_c = 10$		$p_D = 0.75$, $\lambda_c = 4$	
Smoother	CPHD	δ-GLMB	CPHD	δ-GLMB	CPHD	δ-GLMB
G-total	4.64	2.63	6.02	3.76	6.21	3.87
G-Loc	1.17	1.06	1.41	1.39	1.49	1.26
G-Miss	3.49	1.95	4.81	2.99	4.73	2.89
G-False	2.82	1.41	3.32	1.90	3.73	2.17
Time	0.021	0.185	0.024	0.194	0.019	0.174

In the scenario with detection probability $p_D = 0.9$, the clutter number is set to $\lambda_c = 10$; while in the scenario with detection probability $p_D = 0.75$, we set $\lambda_c = 4$. This is detection and clutter (usually assumed to be union of false alarms) are highly interdependent and adjustable via the detection threshold: raising the threshold lowers both detection and false alarm probabilities, and vice-versa [43]. Fig. 2 reveals that the performance gaps between the PHD, MB and the other two smoothers are large, thus we consider only the CPHD and δ-GLMB smoother in this comparison.

Fig. 3 illustrates the mean GOSPA errors of the CPHD and δ-GLMB smoothers. Fig. 3(a) shows that the total GOSPA error of the proposed δ-GLMB smoother is smaller than that of the CPHD smoother. Fig. 3(b) reveals that the δ-GLMB smoother outperforms the CPHD smoother on GOSPA localization error. Besides, compared to the CPHD smoother, the lower GOSPA false and missed targets errors of the proposed smoother in Figs. 3(c) and (d) indicate that it can provide better estimate on target number.

Table 4 provides the root mean square GOSPA errors [26] and execution times of the CPHD and δ-GLMB smoothers over 200 Monte Carlo runs. All codes were written in MATLAB and run on an Intel quad-core processor i5-4590@3.3GHz. It reveals that the δ-GLMB smoother outperforms the CPHD smoother of the same time lag in terms of the GOSPA localization, missed, and false targets errors at the cost of higher computation complexity.

B. SIMULATION 2

We now report the comparison results of the δ-GLMB, LMB [33], and δ-GLMB-A [35] smoothers, and the δ-GLMB filter [17]. A scenario with up to 8 targets is considered here, and all compared smoothers share the lag of one time step.

The standard deviations of the measurement and process noises are $\sigma_w = 2°$, and $\sigma_v = 0.01(°/s^2)$, respectively, and the detection probability and clutter number are $p_D = 0.95$, and $\lambda_c = 16$, respectively. The birth process is a LMB RFS with $\{r_B^{(i)}, p_B^{(i)}\}_{i=1}^{8}$, where the probability of birth is set to $r_B^{(i)} = 0.04$, and the density $p_B^{(i)}(x) = \mathcal{N}(x; \mathbf{m}_B^{(i)}, \mathbf{P}_B)$, with $\mathbf{m}_B^{(i)} = [B^{(i)}, 0, 0]^T$, where $B^{(i)}$ represents the initial bearing of target i, and $\mathbf{P}_B = \mathrm{diag}([4, 0.1, 0.1]^T)$.

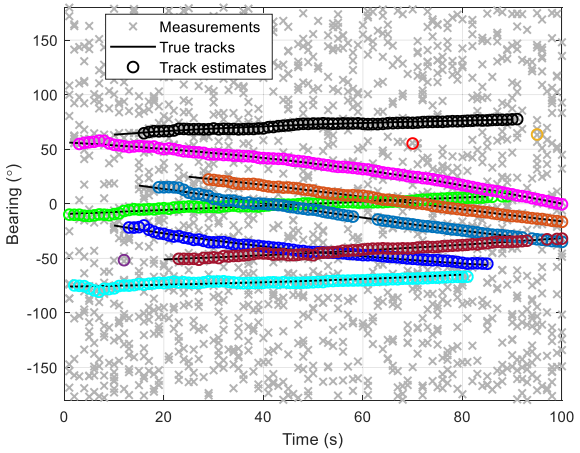

FIGURE 4. A sample run of the proposed smoother for simulation 2.

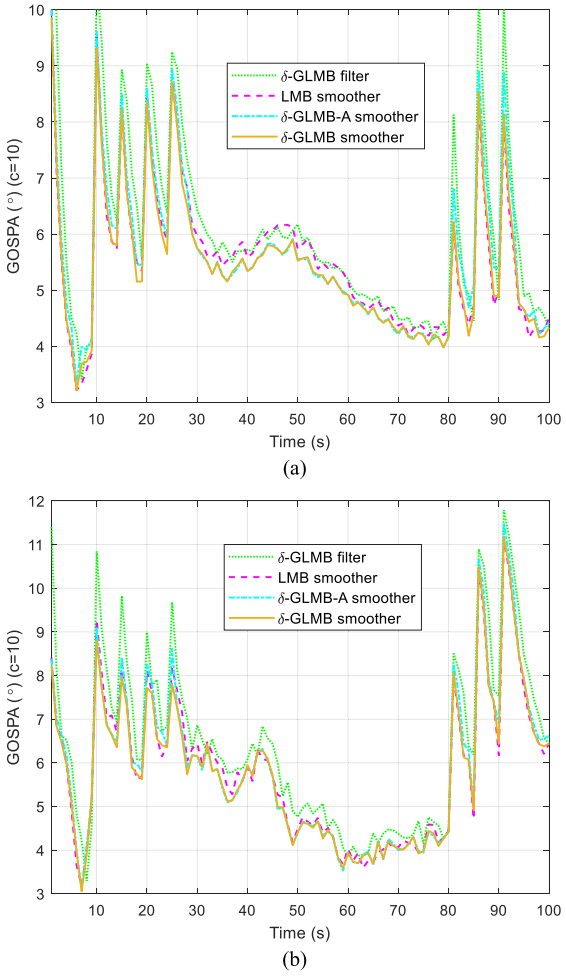

FIGURE 5. Mean GOSPA errors for simulation 2 (200 MC runs). (a) Detection probability 0.95 and clutter number 16, (b) Detection probability 0.75, clutter number 8.

Fig. 4 presents a sample run of the δ-GLMB smoother. In general, the smoother estimates the target number and state well except for few missed points, and due to heavier clutter, false tracks and delay of track initiation and termination also

TABLE 5. Root mean square GOSPA errors for simulation 2.

Setting	$p_D = 0.95$, $\lambda_c = 16$				$p_D = 0.75$, $\lambda_c = 8$			
Smoother/filter	δ-GLMB filter	δ-GLMB-A smoother	LMB smoother	δ-GLMB smoother	δ-GLMB filter	δ-GLMB-A smoother	LMB smoother	δ-GLMB smoother
G-total	6.28	5.76	5.70	5.60	6.72	6.16	6.09	6.01
G-Loc	3.22	2.84	2.86	2.84	3.52	3.14	3.17	3.14
G-Miss	4.63	4.35	4.34	4.21	3.70	3.34	3.33	3.19
G-False	2.74	2.49	2.34	2.36	4.36	4.11	3.99	4.02

exist. No track label switching is observed in this run because of the low process noise level.

Fig. 5 presents the mean GOSPA errors for two different settings. It shows that the δ-GLMB, δ-GLMB-A, and LMB smoothers outperform the δ-GLMB filter, especially when targets births or deaths occur. As to the three smoothers, we observe from Fig. 5 that the δ-GLMB smoother provides the lowest GOSPA error in general, followed by the LMB and δ-GLMB-A smoothers. The GOSPA error of the δ-GLMB-A smoother is almost identical to that of the δ-GLMB smoother, except that it performs less well at the intervals when targets births and deaths occur, because the δ-GLMB-A smoother uses a simplified transition kernel that neglects the births and deaths of targets in the smoothing period.

Table 5 shows that the δ-GLMB smoother outperforms the other three in terms of the root mean square GOSPA error. As expected, the δ-GLMB filter provides the highest GOSPA localization, missed and false target errors. Compared to the LMB smoother, the δ-GLMB smoother provides similar localization and false target errors, while the missed target error of the δ-GLMB smoother is smaller. Compared to the δ-GLMB-A smoother, the δ-GLMB smoother suffers less on missed and false target errors, and the localization errors of both smoothers are very similar.

In summary, the δ-GLMB smoother outperforms the δ-GLMB filter, and the PHD, MB, and CPHD smoothers of the same time lag on estimates of target number and state, and it also outperforms the LMB and δ-GLMB-A smoothers of the same time lag on target number estimate, despite the similar performance of the δ-GLMB, LMB, and δ-GLMB-A smoothers on target state estimate.

C. EXPERIMENT RESULT

We present in this section the experiment result. An experiment with data from an acoustic sensor was conducted. Fig. 6 illustrates the scenario. The sensor (green circle) was fixed at the origin, collecting the bearings of two acoustic targets over the surveillance region, with target 1 (magenta square) moving with nearly constantly velocity and target 2 (blue diamond) fixed at its location.

The measurement is the bearing from sensor to target, referenced clockwise positive to the y-axis, i.e., angle between

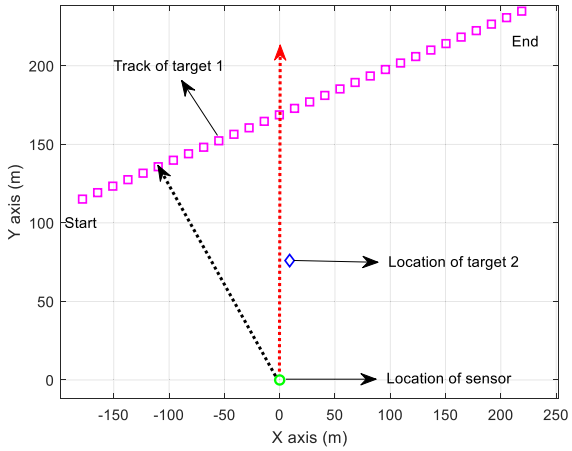

FIGURE 6. Target/sensor geometry of the experiment.

y-axis (red dotted line with arrow) and line of sight (black dotted line with arrow). By turning the power of the acoustic source on or off, we control the birth or death of target. The birth and death of target 1 occur at about 90, and 184 s, and target 2 always exists.

The experiment time is approximately 206s, and the sampling period is $\Delta = 3.3$ s. The standard deviations of the process and measurement noises are set to $\sigma_v = 0.01(^\circ/s^2)$ and $\sigma_w = 2^\circ$. The detection and survival probabilities are set to $p_D = 0.9$ and $p_S = 0.98$. The clutter number is set to $\lambda_c = 6$. The birth process is a LMB RFS with $\{r_B^{(i)}, p_B^{(i)}\}_{i=1}^2$, where $r_B^{(i)} = 0.02$ and $p_B^{(i)}(x) = \mathcal{N}(x; \mathbf{m}_B^{(i)}, \mathbf{P}_B)$, where the covariance matrix $\mathbf{P}_B = \text{diag}([4, 0.1, 0.1]^T)$, and the means $\mathbf{m}_B^{(1)} = [-61, 0, 0]^T$, and $\mathbf{m}_B^{(2)} = [7, 0, 0]^T$.

Fig. 7 shows the tracking results, and Fig. 8 presents the GOSPA errors of the expriment, and Table 6 shows the root mean square GOSPA errors, including the GOSPA localization, missed, and false target errors. Fig. 7 reveals that the CPHD smoother suffers more on missed and false targets, and compared to the δ-GLMB filter, the δ-GLMB smoother performs better on both the estimates of target number and state, as is shown in Table 6. Table 6 also shows that the GOSPA error of the δ-GLMB smoother is smaller than that of the LMB smoother, and the false target error of the LMB smoother is higher due to the unexpected existence of a false track, and the localization error of the δ-GLMB smoother

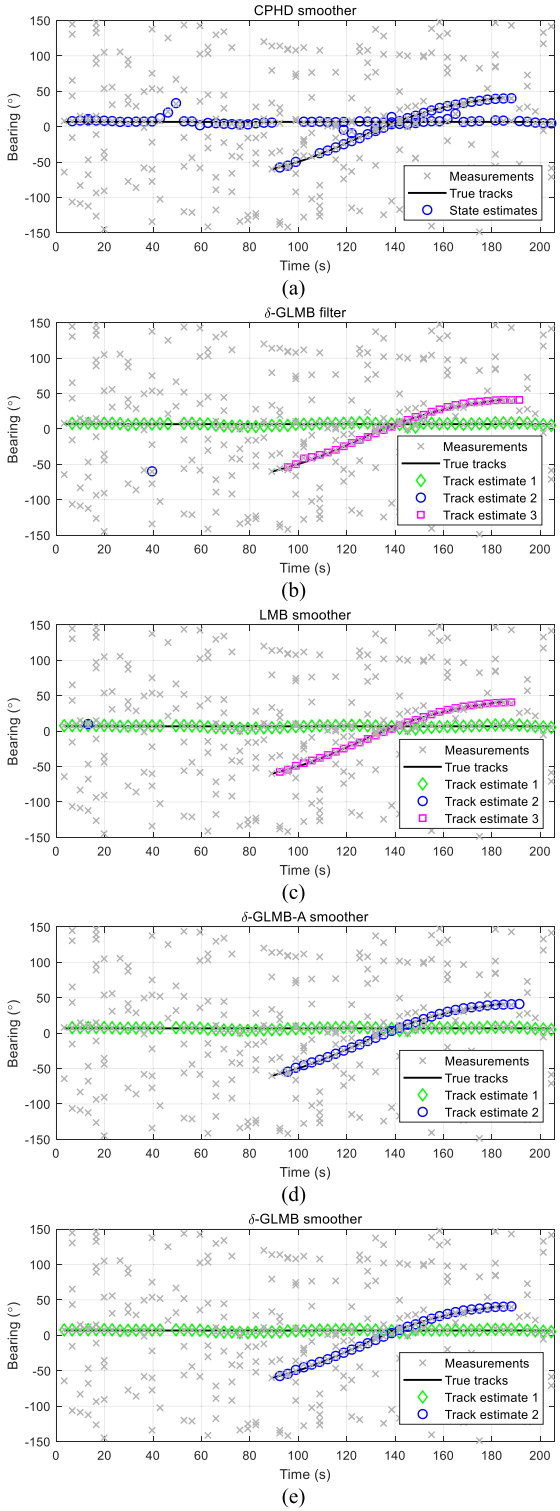

FIGURE 7. Tracking results of the experiment. (a) CPHD smoother, (b) delta-GLMB filter, (c) LMB smoother, (d) delta-GLMB-A smoother, (e) delta-GLMB smoother.

is similar to that of the LMB smoother. The tracking result of the δ-GLMB-A smoother resembles that of the δ-GLMB smoother, except for a small delay of track initiation and termination, which is also reflected by the larger GOSPA error of the δ-GLMB-A smoother at those moments, as is observed from Fig. 8.

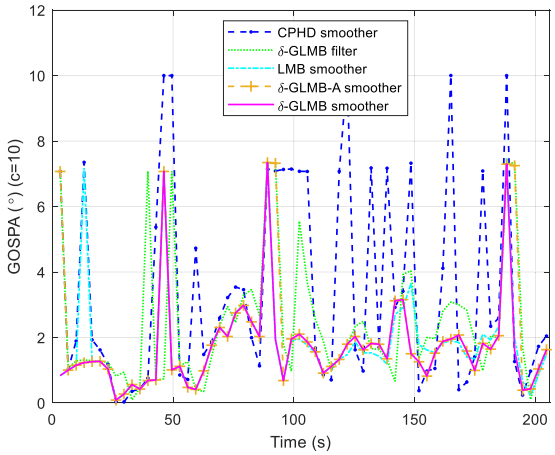

FIGURE 8. GOSPA error of the experiment.

TABLE 6. Root mean square gospa errors of the experiment.

Filter/Smoother	G-Total	G-Loc	G-Miss	G-False
δ-GLMB filter	3.14	2.05	1.79	1.55
CPHD smoother	4.67	1.82	3.23	2.83
δ-GLMB-A smoother	2.71	1.63	1.79	1.27
LMB smoother	2.44	1.65	1.27	1.27
δ-GLMB smoother	2.23	1.63	1.27	0.89

VI. CONCLUSION AND FUTURE RESEARCH

We present a solution for multitarget tracking using one time step lagged δ-GLMB smoothing. By using a formula that resembles the measurement update of the Bayes multitarget filter, we show that a δ-GLMB distributed multitarget filtering density would results in a same distributed one time step lagged multitarget smoothing density. An efficient implementation of the proposed smoother using ranked assignment technique is also given. Numerical results show that the proposed smoothing algorithm outperforms the δ-GLMB filter, and the PHD, MB, and CPHD smoothers of the same time lag on both the estimates of target number and state, and it also outperforms the LMB and δ-GLMB-A smoothers of the same time lag on target number estimate. Future work would consider extending the proposed smoother to the case where the time lag is greater than one.

REFERENCES

[1] Y. Bar-Shalom and X. R. Li, *Multitarget-Multisensor Tracking: Principles and Techniques*. Storrs, CT, USA: YBS Publishing, 1995.
[2] S. Blackman and R. Popoli, *Design and Analysis of Modern Tracking Systems*. Norwood, MA, USA: Artech House, 1999.
[3] G. Pulford, "Taxonomy of multiple target tracking methods," *IEE Proc., Radar Sonar Navig.*, vol. 152, no. 5, p. 291, 2005.
[4] I. Cox and S. Hingorani, "An efficient implementation of Reid's multiple hypothesis tracking algorithm and its evaluation for the purpose of visual tracking," *IEEE Trans. Pattern Anal. Mach. Intell.*, vol. 18, no. 2, pp. 138–150, Feb. 1996.

[5] C. Lundquist, L. Hammarstrand, and F. Gustafsson, "Road intensity based mapping using radar measurements with a probability hypothesis density filter," *IEEE Trans. Signal Process.*, vol. 59, no. 4, pp. 1397–1408, Apr. 2011.

[6] S. H. Rezatofighi, S. Gould, B. T. Vo, B.-N. Vo, K. Mele, and R. Hartley, "Multi-target tracking with time-varying clutter rate and detection profile: Application to time-lapse cell microscopy sequences," *IEEE Trans. Med. Imag.*, vol. 34, no. 6, pp. 1336–1348, Jun. 2015.

[7] R. P. Mahler, *Statistical Multisource-Multitarget Information Fusion*. Norwood, MA, USA: Artech House, 2007.

[8] D. Reid, "An algorithm for tracking multiple targets," *IEEE Trans. Autom. Control*, vol. 24, no. 6, pp. 843–854, Dec. 1979.

[9] T. Fortmann, Y. Bar-Shalom, and M. Scheffe, "Sonar tracking of multiple targets using joint probabilistic data association," *IEEE J. Ocean. Eng.*, vol. 8, no. 3, pp. 173–184, Jul. 1983.

[10] R. Mahler, "Multitarget bayes filtering via first-order multitarget moments," *IEEE Trans. Aerosp. Electron. Syst.*, vol. 39, no. 4, pp. 1152–1178, Oct. 2003.

[11] R. Mahler, "PHD filters of higher order in target number," *IEEE Trans. Aerosp. Electron. Syst.*, vol. 43, no. 99, pp. 1523–1543, Oct. 2007.

[12] B.-T. Vo, B.-N. Vo, and A. Cantoni, "The cardinality balanced multi-target multi-bernoulli filter and its implementations," *IEEE Trans. Signal Process.*, vol. 57, no. 2, pp. 409–423, Feb. 2009.

[13] J. L. Williams, "Marginal multi-bernoulli filters: RFS derivation of MHT, JIPDA, and association-based member," *IEEE Trans. Aerosp. Electron. Syst.*, vol. 51, no. 3, pp. 1664–1687, Jul. 2015.

[14] A. F. Garcia-Fernandez, J. L. Williams, K. Granstrom, and L. Svensson, "Poisson multi-bernoulli mixture filter: Direct derivation and implementation," *IEEE Trans. Aerosp. Electron. Syst.*, vol. 54, no. 4, pp. 1883–1901, Aug. 2018.

[15] D. Clark and J. Bell, "Multi-target state estimation and track continuity for the particle PHD filter," *IEEE Trans. Aerosp. Electron. Syst.*, vol. 43, no. 99, pp. 1441–1453, Oct. 2007.

[16] B.-T. Vo and B.-N. Vo, "Labeled random finite sets and multi-object conjugate priors," *IEEE Trans. Signal Process.*, vol. 61, no. 13, pp. 3460–3475, Jul. 2013.

[17] B.-N. Vo, B.-T. Vo, and D. Phung, "Labeled random finite sets and the Bayes multi-target tracking filter," *IEEE Trans. Signal Process.*, vol. 62, no. 24, pp. 6554–6567, Dec. 2014.

[18] R. Mahler, "A brief survey of advances in random-set fusion," in *Proc. Int. Conf. Control, Autom. Inf. Sci. (ICCAIS)*, Oct. 2015, pp. 62–67.

[19] B.-N. Vo, B.-T. Vo, and H. G. Hoang, "An efficient implementation of the generalized labeled multi-Bernoulli filter," *IEEE Trans. Signal Process.*, vol. 65, no. 8, pp. 1975–1987, Apr. 2017.

[20] S. Reuter, B. T. Vo, B. N. Vo, and K. Dietmayer, "The labeled multi-Bernoulli filter," *IEEE Trans. Signal Process.*, vol. 62, no. 12, pp. 3246–3260, Dec. 2014.

[21] C. Fantacci and F. Papi, "Scalable multisensor multitarget tracking using the marginalized δ-GLMB density," *IEEE Signal Process. Lett.*, vol. 23, no. 6, pp. 863–867, Jun. 2016.

[22] M. Beard, B.-T. Vo, and B.-N. Vo, "Bayesian multi-target tracking with merged measurements using labelled random finite sets," *IEEE Trans. Signal Process.*, vol. 63, no. 6, pp. 1433–1447, Mar. 2015.

[23] M. Beard, S. Reuter, K. Granstrom, B.-T. Vo, B.-N. Vo, and A. Scheel, "Multiple extended target tracking with labeled random finite sets," *IEEE Trans. Signal Process.*, vol. 64, no. 7, pp. 1638–1653, Apr. 2016.

[24] S. Li, W. Yi, R. Hoseinnezhad, B. Wang, and L. Kong, "Multiobject tracking for generic observation model using labeled random finite sets," *IEEE Trans. Signal Process.*, vol. 66, no. 2, pp. 368–383, Jan. 2018.

[25] A. F. Garcia-Fernandez and L. Svensson, "Trajectory PHD and CPHD filters," *IEEE Trans. Signal Process.*, vol. 67, no. 22, pp. 5702–5714, Nov. 2019.

[26] A. F. Garcia-Fernandez, L. Svensson, and M. R. Morelande, "Multiple target tracking based on sets of trajectories," *IEEE Trans. Aerosp. Electron. Syst.*, to be published.

[27] B. D. O. Anderson and J. B. More, *Optimal Filtering*. Englewood Cliffs, NJ, USA: Prentice-Hall, 1979.

[28] R. P. S. Mahler, B.-T. Vo, and B.-N. Vo, "Forward-backward probability hypothesis density smoothing," *IEEE Trans. Aerosp. Electron. Syst.*, vol. 48, no. 1, pp. 707–728, Jan. 2012.

[29] N. Nadarajah, T. Kirubarajan, T. Lang, M. Mcdonald, and K. Punithakumar, "Multitarget tracking using probability hypothesis density smoothing," *IEEE Trans. Aerosp. Electron. Syst.*, vol. 47, no. 4, pp. 2344–2360, Oct. 2011.

[30] D. Li, C. Hou, and D. Yi, "Multi-Bernoulli smoother for multi-target tracking," *Aerosp. Sci. Technol.*, vol. 48, pp. 234–245, Jan. 2016.

[31] S. Nagappa, E. D. Delande, D. E. Clark, and J. Houssineau, "A tractable forward–backward CPHD smoother," *IEEE Trans. Aerosp. Electron. Syst.*, vol. 53, no. 1, pp. 201–217, Feb. 2017.

[32] M. Beard, B. T. Vo, and B. N. Vo, "Generalised labelled multi-Bernoulli forward-backward smoothing," in *Proc. 19th Int. Conf. Inf. Fusion*, Heidelberg, Germany, Jul. 2016, pp. 688–694.

[33] R. Liu, H. Fan, T. Li, and H. Xiao, "A computationally efficient labeled multi-Bernoulli smoother for multi-target tracking," *Sensors*, vol. 19, no. 19, p. 4226, Sep. 2019.

[34] T. Nguyen and D. Kim, "GLMB tracker with partial smoothing," *Sensors*, vol. 19, no. 20, p. 4419, Oct. 2019.

[35] Q.-R. Li, B. Qi, and G.-L. Liang, "Approximate Bayes multi-target tracking smoother," *IET Radar, Sonar Navigat.*, vol. 13, no. 3, pp. 428–437, Mar. 2019.

[36] B. N. Vo, B. T. Vo, and R. P. Mahler, "Closed-form solutions to forward–backward smoothing," *IEEE Trans. Signal Process.*, vol. 60, no. 1, pp. 2–17, Sep. 2011.

[37] K. G. Murty, "An algorithm for ranking all the assignments in order of increasing cost," *Oper. Res.*, vol. 16, pp. 682–687, Mar. 1968.

[38] B.-T. Vo, B.-N. Vo, and A. Cantoni, "Analytic implementations of the cardinalized probability hypothesis density filter," *IEEE Trans. Signal Process.*, vol. 55, no. 7, pp. 3553–3567, Jul. 2007.

[39] D. Schuhmacher, B.-T. Vo, and B.-N. Vo, "A consistent metric for performance evaluation of multi-object filters," *IEEE Trans. Signal Process.*, vol. 56, no. 8, pp. 3447–3457, Aug. 2008.

[40] A. S. Rahmathullah, A. F. Garcia-Fernandez, and L. Svensson, "Generalized optimal sub-pattern assignment metric," in *Proc. 20th Int. Conf. Inf. Fusion (Fusion)*, Jul. 2017, pp. 1–8.

[41] Y. Bar-Shalom, X.-R. Li, and T. Kirubarajan, *Estimation with Applications to Tracking and Navigation*. Hoboken, NJ, USA: Wiley, 2001.

[42] D. Franken, M. Schmidt, and M. Ulmke, "'Spooky action at a distance' in the cardinalized probability hypothesis density filter," *IEEE Trans. Aerosp. Electron. Syst.*, vol. 45, no. 4, pp. 1657–1664, Oct. 2009.

[43] T. Fortmann, Y. Bar-Shalom, M. Scheffe, and S. Gelfand, "Detection thresholds for tracking in clutter–A connection between estimation and signal processing," *IEEE Trans. Autom. Control*, vol. 30, no. 3, pp. 221–229, Mar. 1985.

GUOLONG LIANG was born in 1964. He received the B.E., M.S., and Ph.D. degrees from Harbin Engineering University, Harbin, China, in 1988, 1991, and 1997, respectively. He is currently a Professor with the College of Underwater Acoustic Engineering, Harbin Engineering University. His research interests include underwater target detection, localization, tracking, and navigation.

QUANRUI LI was born in 1989. He received the B.E. degree in electronic and information engineering from Harbin Engineering University, Harbin, China, in 2012, where he is currently pursuing the Ph.D. degree with the College of Underwater Acoustic Engineering. His research interests include the random finite set, multitarget tracking, nonlinear filtering, and data fusion.

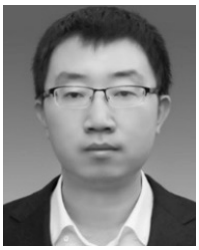

BIN QI was born in 1985. He received the Ph.D. degree from Harbin Engineering University, Harbin, China. He is currently an Associate Professor with the College of Underwater Acoustic Engineering, Harbin Engineering University. His main research interests include underwater target tracking and target motion analysis.

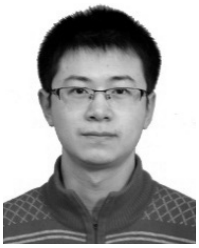

LONGHAO QIU was born in 1988. He received the B.E. and Ph.D. degrees from Harbin Engineering University, Harbin, China, in 2011 and 2018, respectively. He is currently a Reach Worker with the College of Underwater Acoustic Engineering, Harbin Engineering University. His main research interests include array signal processing and target tracking.